# Nonadiabatic instanton calculation of multistate electron transfer reaction rate: Interference effects in three and four states systems

Seogjoo Jang and Jianshu Cao[a)]
*Department of Chemistry, Massachusetts Institute of Technology, Cambridge, Massachusetts 02139*

(Received 14 December 2000; accepted 21 March 2001)

For multistate electron transfer reactions with quantum reaction coordinates, nonadiabatic instanton theory can provide a powerful and direct means of calculating the reaction rate without any limitation to the magnitudes of electronic coupling constants. In order to examine its performance in detail, the theory is applied to simple model systems with three and four electronic states which have one and two bridge states respectively. Calculations for three states systems, varying the through–bond coupling constant, show that the nonadiabatic instanton theory reproduces the results of perturbation and adiabatic instanton theories in the limits of small and large coupling constants, respectively. In the absence of through–space coupling, the crossover between the two limits is smooth and monotonic. However, in the presence of through–space coupling, the crossover pattern becomes sensitive to the relative phase of the two electronic channels and demonstrates substantial interference effects. For a four states system that has two interfering through–bond coupling paths, similar interference effect was observed. These results show that the nonadiabatic instanton method can serve as a favorable means of understanding the general kinetics and exploring the interference effects in the low-temperature bridge mediated and/or proton coupled electron transfer systems.  [DOI: 10.1063/1.1371262]

## I. INTRODUCTION

Electron transfer (ET) reaction assumes a central role in various chemical and biological processes. In each situation, a proper characterization of ET forms an essential step towards fundamental understandings of the underlying mechanism. Recent reviews[1–3] provide the general perspective of numerous successful theories, extensive examples of ET that can be well explained by existing theories, and some remaining problems where the theoretical issues have not been resolved yet. One of these latter fields where active theoretical efforts are currently under way, is multistate ET coupled to quantum modes. Typical examples in this category can be found from intramolecular ET involving synthetic organic (or organometallic) compounds,[2] multicenter ET in biological systems,[1,4–7] ET across an adsorbate in heterogeneous media,[1,3] and proton coupled ET (PCET).[8]

Important features of multistate quantum ET can be captured by theories based on simplified model potentials.[1,3] Especially, in the weak coupling limit, kinetic and mechanistic aspects are well described by perturbation analysis. However, as revealed by some recent experiments and *ab initio* calculations,[9,10] quantitative estimation of the reaction rate, considering all the microscopic details of a given reactive system, remains difficult in most cases, due to complicated potential-energy surfaces and collective nonlinear reaction coordinates. For these systems, it is not always clear whether all the electronic couplings are weak enough to warrant perturbation analysis. In addition, interference effects[11–13] and the dynamic role of quantum reaction coordinates may turn out to be important.

Among the various examples of quantum ET, systems of PCET have relatively well defined characteristics and have been subject to extensive studies.[8,14–26] Of particular biological importance is the case where the proton moiety functions as a hydrogen bond bridge,[8] making the ET reaction more efficient. A great deal of understandings have been achieved through a series of elegant experimental studies by Nocera and co-workers.[8,14–16] Cukier has laid an important theoretical framework for this type of PCET, explaining experimentally observed isotope effects and clarifying important conceptual issues such as sequentiality and concertedness of the reaction mechanism.[8,17,18] Later, he developed a dielectric continuum theory,[8,18,19] where both electron and proton are treated on the same footing, resulting in one-dimensional multistate system. Soudackov and Hammes-Schiffer[20,21] improved upon this perspective by formulating a two-dimensional dielectric continuum theory, which can be applied to more general situations. Recent applications[22] of their theory to model systems demonstrate its capacity in explaining rich behavior. However, in both theories, a reliable calculation of the reaction rate seems limited to the weak electronic coupling regime.

In more complicated situations of PCET,[23–26] protons are actively involved in substantial molecular rearrangements, bond breaking, and bond formation. In these cases, proton degrees of freedom play a more active role as the reaction coordinate, and various behavior can emerge depending on the number and topology of different charge localization centers. In addition, the overall reaction may involve substantial tunneling of proton as well as of electron, with the resulting isotope effects varying with the specifics of systems.[23–26] For example, a recent experiment[26] reports a

[a)]Electronic mail: jianshu@mit.edu

 

kinetic isotope effect of 41.4, which is quite large compared to those for systems involving protons in hydrogen bond bridge moiety only. Theoretical calculation of the reaction rate for these general situations is more challenging, because nonlinearity of the reaction coordinate and quantum effects such as tunneling, nonadiabaticity, and interference need to be considered.

As illustrated by the PCET systems described above, developing a unified theoretical framework, applicable to systems with general reaction coordinates and arbitrary strength of coupling, is crucial for understanding a broad class of multistate quantum ET systems. To this end, one may extend some analytic theories[27–32] into more general situations, as have been done for several three states problems,[33–36] or utilize various successful path integral simulation,[37,38] semiclassical dynamics,[39–43] and mixed quantum classical dynamics approaches.[37,44–47] In the present work, we seek another possibility of employing the nonadiabatic instanton theory, which has been proposed by Cao and Voth (CV)[48,49] and improved by Schwieters and Voth (SV)[50] in a more consistent form later.

Nonadiabatic instanton theory[48–50] is a multistate generalization of the original instanton theory[51–57] for a single potential-energy surface. It can be applied whenever the nuclear trajectory is coupled to discrete electronic states and there are bottleneck regions which form effective barriers of nuclear tunneling. The main idea involved in this extension is similar to that[58,59] of an open system, where the extra degrees of freedom are included as influence functional and the equation of motion becomes nonlocal in time. Although some earlier studies[60–62] had assumed this idea implicitly in analogy with Pechukas' real time dynamics theory,[39] it was the systematic exposition and thorough numerical studies made by CV[48,49] and later by SV,[50] which brought it into a well-established methodology.

The nonadiabatic instanton calculation does not presupposes weak coupling or classical limit of the reaction coordinate. Therefore, as long as temperature is sufficiently low, its application is warranted for a general class of systems. However, there are certain assumptions involved in the theory. Most importantly, it presupposes that a given reaction can be characterized by noninterfering nuclear tunneling trajectories. As a result, nuclear coherence cannot be accounted for within that approach,[59] which might be a critical factor if the symmetry of the system allows degenerate nuclear tunneling trajectories. On the other hand, the effects of electronic interference along a given nuclear trajectory is inherent in the formalism, which is an essential motivation in applying the theory to multistate systems.

Although the nonadiabatic instanton theory[48–50] has been formulated for an arbitrary number of states, calculations have been performed only for systems with two electronic states. The present paper goes beyond these examples and extends the nonadiabatic instanton method to three and four states systems. For two states systems, the theory reproduces the correct behavior in the limits of small and large coupling constants. These properties can be examined in the multistate systems. In addition, for the present case, more electronic paths connecting the initial donor and the final acceptor states coexist, and the interference among them can result in rich kinetic behavior. The main concern is whether the nonadiabatic instanton theory captures such effects. Tests of these two aspects form important criteria that can validate the application of the theory to real systems. In order to keep other features as simple as possible, we limit the nuclear coordinate to one dimension, although calculation for at least two-dimensional nuclear coordinates is feasible and has been done before.[50]

The sections are organized as follows. Section II presents the formulation of the nonadiabatic instanton theory. Section III provides results for model three and four states systems, and demonstrates that the desired properties are satisfied. The paper concludes with several discussions in Sec. IV, which address physical implications of the present results and future directions of the theory.

## II. UNIFIED FORMULATION

The formulation of the nonadiabatic instanton theory is provided in the present section. The starting expression and formal development is different from previous ones.[48–50] We follow the traditional approach that includes the adiabatic instanton theory as a limiting situation.[52–56] But the final rate expression is equivalent to that provided by SV,[50] when put into a discretized form.

For large barrier and low temperature, the decay rate of a metastable state[52–56] is given by

$$\Gamma = \frac{2}{\beta\hbar}\frac{\mathrm{Im}\, Z}{Z_r}, \tag{1}$$

where $Z_r$ is the reactant part of the partition function, and $Z$ is analytically continued complex partition function of the total reactive system. The physical and mathematical meanings of these terms are well-known in the adiabatic instanton theory,[52–56] and similar definitions are possible for the present case as will become clear later.

The total reactive system consists of one dimensional nuclear coordinate and discrete electronic states. Formally, one can express the partition function of the total system as

$$Z = \int dq_0 \cdots \int dq_{N-1} \sum_{k_0} \cdots \sum_{k_{N-1}} \langle q_0|\langle k_0|e^{-\epsilon \hat{H}}|k_1\rangle|q_1\rangle \times \cdots \langle q_{N-1}|\langle K_{N-1}|e^{-\epsilon \hat{H}}|k_N\rangle|q_N\rangle, \tag{2}$$

for an arbitrary $N$. In above equation, $\epsilon = \beta/N$ and the cyclic boundary condition of $q_N = q_0$ and $k_N = k_0$ was imposed. $|q_j\rangle$ represents a position state of the continuous nuclear degree of freedom, and $|k_j\rangle$ a discrete electronic state. $\hat{H}$ is the total system Hamiltonian given by

$$\hat{H} = \hat{H}_0 + \hat{H}_1, \tag{3}$$

where

$$\hat{H}_0 = \frac{\hat{p}^2}{2m}\hat{I} + \sum_{k=1}^{M}\sum_{l\neq k}\Delta_{kl}|k\rangle\langle l|, \tag{4}$$

$$\hat{H}_1 = \sum_{k=1}^{M} V_k(\hat{q})|k\rangle\langle k|. \tag{5}$$

In Eq. (4), $\hat{I}$ is the identity operator in the space of electronic states with the dimension of $M$. It is assumed that the coupling matrix elements of $\Delta_{kl}$ are real and symmetric. In Eq. (5), $V_k(q)$ represents the diabatic potential-energy surface of the $k$th electronic state.

By convention, we define $|1\rangle$ as the reactant (donor) state and $|M\rangle$ as the product (acceptor) state. It is assumed that the nuclear coordinate $q$ can serve as a good criterion for the distinction of these two states. Specifically, it is assumed that there are two disjoint sets of $S_r$ and $S_p$ and that the Boltzmann factor of state $|1\rangle$ ($|M\rangle$) is dominantly larger than those of others if $q \in S_r(S_p)$. In this sense, the rate for the nuclear trajectory to tunnel from the region of $S_r$ to $S_p$, can always be identified as the electron transfer rate from state $|1\rangle$ to $|M\rangle$, irrespective of the magnitudes of the electronic coupling constants.

A path integral expression for the partition function of Eq. (2) can be obtained using the following approximation:

$$\begin{aligned}\langle q'|\langle k'|e^{-\epsilon\hat{H}}|k''\rangle|q''\rangle &\approx \langle q'|\langle k'|e^{-\epsilon\hat{H}_1/2}e^{-\epsilon\hat{H}_0}e^{-\epsilon\hat{H}_1/2}|k''\rangle|q''\rangle \\ &= \sqrt{\frac{m}{2\epsilon\hbar^2}}\exp\left\{-\frac{m}{2\epsilon\hbar^2}(q'-q'')^2\right\}J_{k',k''}(q',q'';\epsilon),\end{aligned} \tag{6}$$

where

$$\begin{aligned}J_{k',k''}(q',q'';\epsilon) \equiv e^{-\epsilon V_{k'}(q')/2}\langle k'|e^{-\epsilon\Sigma_{k\neq l}\Delta_{kl}|k\rangle\langle l|}|k''\rangle \\ \times e^{-\epsilon V_{k''}(q'')/2}.\end{aligned} \tag{7}$$

We define an operator $\hat{J}(q',q'';\epsilon)$ in the space of electronic states, with the components given by Eq. (7). In the limit of $N\to\infty$, we also define the following electronic influence functional operator:

$$\hat{J}[q(\cdot);\tau',\tau''] \equiv \lim_{N\to\infty}\hat{J}(q_{j'},q_{j'+1};\epsilon)\cdots\hat{J}(q_{j''-1},q_{j''};\epsilon), \tag{8}$$

where $\tau' = j'\epsilon$ and $\tau'' = j''\epsilon$. Taking the limit of $N\to\infty$ in Eq. (2) and utilizing the above definition of Eq. (8), one can obtain the following path integral expression for the partition function:

$$Z = \int \mathcal{D}q(\cdot)e^{-1/\hbar\int_0^{\beta\hbar}d\tau m\dot{q}(\tau)^2/2}J[q(\cdot)], \tag{9}$$

with

$$J[q(\cdot)] \equiv \mathrm{Tr}_e\{\hat{J}[q(\cdot);0,\beta\hbar]\}, \tag{10}$$

where $Tr_e$ is the trace over electronic states.

The electronic influence functional defined by Eq. (10) is positive definite. Taking a logarithm and expanding around a path of $q_0(\cdot)$ up to the second order, one can approximate it as

$$\begin{aligned}\ln(J[q(\cdot)]) \approx \ln(J[q_0(\cdot)]) - \frac{1}{\hbar}\int_0^{\beta\hbar}d\tau\langle V'(\tau)\rangle_{q_0(\cdot)}\delta q(\tau) \\ - \frac{1}{2\hbar}\int_0^{\beta\hbar}d\tau\langle V''(\tau)\rangle_{q_0(\cdot)}\delta q(\tau)^2 + \frac{1}{2\hbar^2} \\ \times\int_0^{\beta\hbar}d\tau\int_0^{\beta\hbar}d\tau' C[q_0(\cdot);\tau,\tau']\delta_q(\tau)\delta_q(\tau'),\end{aligned} \tag{11}$$

where

$$\begin{aligned}\langle V'(\tau)\rangle_{q_0(\cdot)} \equiv \frac{1}{J[q_0(\cdot)]}Tr_e\{\hat{J}[q_0(\cdot);0,\tau]\hat{V}'(q_0(\tau)) \\ \times\hat{J}[q_0(\cdot);\tau,\beta\hbar]\}\end{aligned} \tag{12}$$

with

$$(\hat{V}'(q_0(\tau)))_{j,k} = \delta_{j,k}V_k'(q_0(\tau)). \tag{13}$$

In Eq. (11), $\langle V''(\tau)\rangle_{q_0(\cdot)}$ is defined in a way similar to Eq. (12), and

$$\begin{aligned}C[q_0(\cdot);\tau,\tau'] \equiv \langle V'(\tau)V'(\tau')\rangle_{q_0(\cdot)} - \langle V'(\tau)\rangle_{q_0(\cdot)} \\ \times\langle V'(\tau')\rangle_{q_0(\cdot)}, \quad \tau\neq\tau',\end{aligned} \tag{14}$$

with

$$\begin{aligned}\langle V'(\tau)V'(\tau')\rangle_{q_0(\cdot)} \equiv \frac{1}{J[q_0(\cdot)]}Tr_e\{\hat{J}[q_0(\cdot);0,\tau_<] \\ \times\hat{V}'(q_0(\tau_<))\hat{J}[q_0(\cdot);\tau_<,\tau_>] \\ \times\hat{V}'(q_0(\tau_>))\hat{J}[q_0(\cdot);\tau_>,\beta\hbar]\},\end{aligned} \tag{15}$$

where $\tau_< = \min(\tau,\tau')$ and $\tau_> = \max(\tau,\tau')$. It is important to recognize that the average quantities defined above are all functionals of the path $q_0(\cdot)$.

Expanding the kinetic-energy term in Eq. (9), and combining with the expansion of Eq. (11), one can show that the first-order terms in the functional expansion of the partition function vanish and only the quadratic terms survive, around the path satisfying the following ''classical'' equation of motion:

$$m\ddot{q}_0(\tau) = \langle V'(\tau)\rangle_{q_0(\cdot)}. \tag{16}$$

Given that there are more than one such trajectories and they are well separated from each other, the partition function of Eq. (9) can be approximated as

$$\begin{aligned}Z \approx \sum_{q_0(\cdot)} e^{-1/\hbar\int_0^{\beta\hbar}d\tau m\dot{q}_0(\tau)^2/2}J[q_0(\cdot)]\int\mathcal{D}\delta q(\cdot) \\ \times\exp\left\{-\frac{1}{2\hbar}\int_0^{\beta\hbar}d\tau\delta q(\tau)D[q_0(\cdot);\tau]\delta q(\tau)\right\},\end{aligned} \tag{17}$$

where $D[q_0(\cdot):\tau]$ is an integro-differential operator defined by

$$D[q_0(\cdot);\tau]f(\tau)\equiv\{-m\partial_\tau^2+\langle V''(\tau)\rangle_{q_0(\cdot)}\}f(\tau) - \frac{1}{\hbar}\int_0^{\beta\hbar} d\tau' C[q_0(\cdot);\tau,\tau']f(\tau'), \quad (18)$$

with $f(\tau)$ being an arbitrary periodic function.

The ''classical'' trajectories of $q_0(\cdot)$'s satisfying Eq. (16) should be periodic in $\tau$ with the period of $\beta\hbar$. Trivial solutions with this nature are constant trajectories. The reactant part of the partition function comes from expansion around one such constant solution, locally maximizing $J[q(\cdot)]$ within the reactant region of $S_r$. In order to find this constant solution, we first introduce the following effective potential:

$$V_e(q)=-\frac{1}{\beta}\ln(J[q]), \quad (19)$$

which is defined only for the class of constant trajectories, $q(\cdot)=q$. Then,

$$V_e'(q)=\langle V'(\tau)\rangle_q. \quad (20)$$

If one defines $q_r$ as the position of the local minimum of $V_e(q)$ in the reactant region $S_r$, then $\langle V'(\tau)\rangle_{q_r}=V_e'(q_r)=0$. That is, $q(\tau)=q_r$ is a constant solution of Eq. (16). As a result, the reactant part of the partition function becomes

$$Z_r=J[q_r]\int \mathcal{D}\delta q(\cdot) \times\exp\left\{-\frac{1}{2\hbar}\int_0^{\beta\hbar} d\tau\delta q(\tau)D[q_r;\tau]\delta q(\tau)\right\}. \quad (21)$$

Since $D[q_r,\tau]$ is positive definite, the above path integral amounts to stable Gaussian integrals and can be integrated to be

$$Z_r=J[q_r]\frac{\mathcal{N}}{\Pi_n\sqrt{\Lambda_n^r}}, \quad (22)$$

where $\mathcal{N}$ is a normalization constant and $\Lambda_n^r$'s are eigenvalues of the operator, $D[q_r;\tau]$.

The barrier part of the partition function is defined as the semiclassical expansion around the trajectories which join or coexist in $S_r$ and $S_p$. We assume that the temperature and topology of the potential allows existence of nontrivial periodic trajectories with period $\beta\hbar$, and that there is one dominant trajectory, denoted as $q_b(\tau)$, with the smallest action. Then, the barrier part of the partition function can be approximated as

$$Z_b\approx e^{-1/\hbar\int_0^{\beta\hbar}d\tau m\dot{q}_b(\tau)^2/2}J[q_b(\cdot)]\int \mathcal{D}\delta q(\cdot) \times\exp\left\{-\frac{1}{2\hbar}\int_0^{\beta\hbar} d\tau\delta q(\tau)D[q_b(\cdot);\tau]\delta q(\tau)\right\}. \quad (23)$$

Unlike $D[q_r;\tau]$,$D[q_b(\cdot);\tau]$ has a nontrivial zero eigenvalue solution, $\dot{q}_b(\cdot)$. This solution has one node, and there should be an additional solution of the operator $D[q_b(\cdot);\tau]$, which has no node and a negative eigenvalue. The above integral diverges due to this negative eigenvalue mode. However, as is done for adiabatic instanton theory,[51–57] a proper analytic continuation leads to the following imaginary value:

$$Z_b=\frac{i\beta\hbar}{2}\sqrt{\frac{W_b}{2\pi\hbar}}\frac{\mathcal{N}}{\Pi_n'\sqrt{|\Lambda_n^b|}}e^{-1/2\hbar W_b}J[q_b(\cdot)], \quad (24)$$

where $\Lambda_n^b$'s are eigenvalues of $D[q_b(\cdot);\tau]$, the prime in the product means excluding the zero eigenvalue, and

$$W_b=m\int_0^{\beta\hbar} d\tau\dot{q}_b^2(\tau). \quad (25)$$

Inserting Eqs. (22) and (24) into Eq. (1), the decay rate is given by

$$\Gamma=\sqrt{\frac{W_b}{2\pi\hbar}}\left(\frac{\Pi_n\Lambda_n^r}{\Pi_n'|\Lambda_n^b|}\right)^{1/2}e^{-1/2\hbar W_b}J[q_b(\cdot)]/J[q_r], \quad (26)$$

which corresponds to the nonadiabatic generalization of the adiabatic instanton theory. This is the main formal result of the present paper. Previously, only the discretized version was reported.[50]

## III. RESULTS FOR MODEL SYSTEMS

In the present section, the results of calculation for model systems are provided. A discretized version of Eq. (26) is used as described in Appendix A, with $N=200$. In order to compare easily with the perturbation theory, we assume all the diabatic potential-energy surfaces are those of shifted or displaced harmonic oscillators with the same frequency of $\omega$. The mass of the $q$ coordinate is denoted as $m$. In all the calculations, the units were chosen such that $m=\omega=\hbar=1$, and $\beta=10$ in these units.

Before going through the main results, it is meaningful to provide some estimates of the units and temperature chosen here. If one assumes that the mass is equal to that of proton and the well frequency is equal to 2000 $cm^{-1}$, the corresponding units of mass and time are $1.7\times10^{-24}$ g and $1.7\times10^{-14}$ s. In order to make $\hbar=1$, the remaining unit of length should be equal to 0.32 Å. The Boltzmann constant in these units have the value of $2.2\times10^{-3}$, and $\beta=10$ corresponds to $T=45$ K. Thus, we are concerned here in a very low-temperature regime. This choice was made in order to ensure that there exists instanton solution over the broad range of coupling constants considered. In actual systems where the coupling constant is in a small limited range, the temperature one can apply the present method might be higher.

### A. Three states system without through–space coupling

A three state system consisting of $|1\rangle$, $|2\rangle$, and $|3\rangle$ is considered. $|1\rangle$ corresponds to the donor state and $|3\rangle$ to the acceptor state. There is no direct coupling between $|1\rangle$ and $|3\rangle$, i.e., no through–space coupling, and it is assumed that the coupling between $|1\rangle$ and $|2\rangle$ is the same as that between $|2\rangle$ and $|3\rangle$, which is denoted as $\Delta$ (through–bond coupling constant). The present model thus corresponds to an idealized version of symmetric bridge mediated ET[1,3] without direct interaction between the donor and acceptor states due to

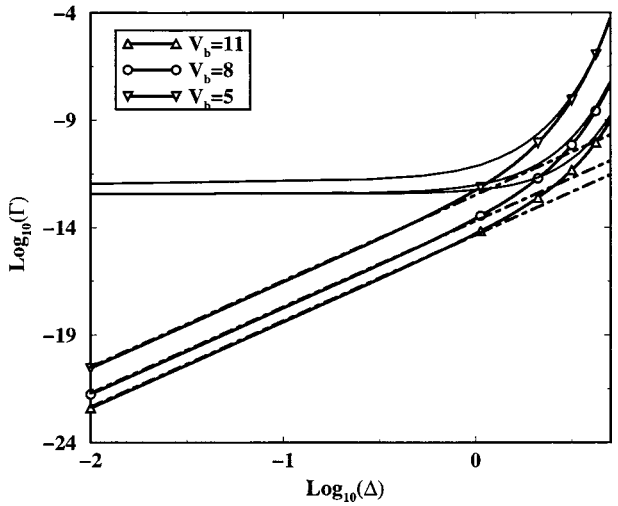


FIG. 1. Nonadiabatic instanton rates for three cases of bridge state potential: $V_b=11$, 8, and 5. The second-order perturbation results are shown as dotted–dashed lines, and the adiabatic instanton results are shown as thin solid lines.

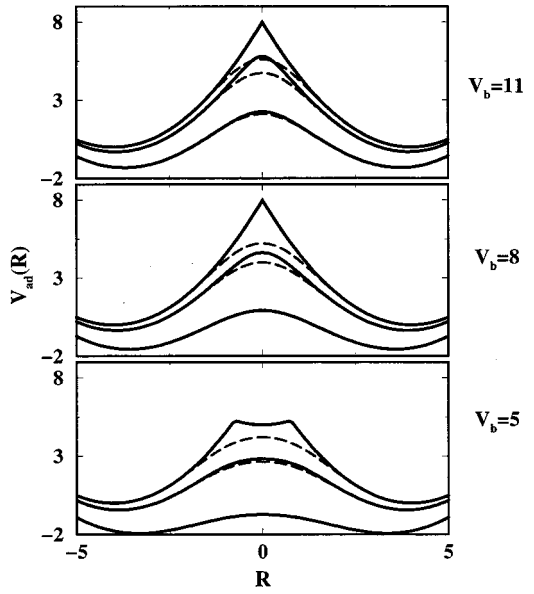


FIG. 2. The lowest adiabatic potential-energy surfaces (solid lines) for three values of Δ: 0.01, 2.37, and 5. For each case of $V_b$, the higher potential-energy surface corresponds to the smaller value of Δ. Long dashed lines are the effective potential-energy surfaces calculated by Eq. (31).

either large distance or symmetry reason. The quantum reaction coordinate in the present case can be considered as collective polarization coordinate in the low-temperature limit and/or the proton coordinate, depending on the type of a given system.

The form of $\hat{H}_0$ of Eq. (4), for the present case, is given by

$$\hat{H}_0=\frac{\hat{p}^2}{2m}\hat{I}+\Delta(|1\rangle\langle 2|+|2\rangle\langle 1|+|2\rangle\langle 3|+|3\rangle\langle 2|). \quad (27)$$

The diabatic potential-energy surfaces entering $\hat{H}_1$ of Eq. (5) are given by

$$V_1(q)=\frac{m\omega^2}{2}(q+q_0)^2, \quad (28)$$

$$V_2(q)=\frac{m\omega^2}{2}q^2+V_b, \quad (29)$$

$$V_3(q)+\frac{m\omega^2}{2}(q-q_0)^2, \quad (30)$$

where $q_0=4$. In the units estimated above, this corresponds to about 1.28 Å. Thus our model represent situations where substantial bond rearrangements occur.

Calculations were done with three different choices of $V_b=11$, 8, and 5 in $V_2(q)$ of Eq. (29). Figure 1 shows the reaction rates with the variation of Δ, from 0.01 to 5. Also shown are the results based on the second-order perturbation theory as described in Appendix B and the adiabatic instanton theory results for the lowest adiabatic potential-energy surfaces. The apparent values of the reaction rates look very small. However, considering that the unit time scale as estimated above is on the order of $10^{-14}$ s, the range of the reaction rates covers experimentally relevant time scales. In the weak coupling limit, the nonadiabatic instanton theory results agree with those of the perturbation theory. As the coupling constant increases, they approach those of the adiabatic instanton theory, the quantum limit of adiabatic ET theory. Thus it is shown that the nonadiabatic instanton theory interpolates the nonadiabatic regime and the true adiabatic regime, which accounts for the lowering of the effective nuclear barrier height and thus has much larger rate than the adiabatic limit of the Landau–Zenner expression. As in the case of two electronic states,[48–50] the crossover is smooth and monotonic.

The effects of the variation of the bridge state potential on the reaction rates can be clearly seen in Fig. 1. First, the relative rates for different values of $V_b$ are quite insensitive to the magnitudes of the coupling constant, Δ. Second, larger values of $V_b$ tend to delay the crossover to the adiabatic limit. Qualitatively, however, the three curves show similar pattern. This is somewhat in contrast to the adiabatic instanton theory results, for which the reaction rates for the cases of $V_b=8$ and $V_b=11$ approach each other quite closely as Δ decreases. Figure 2 shows the lowest adiabatic potential-energy surfaces for three values of Δ and these seem to explain the observed trend. The lowest adiabatic surfaces for the two cases of $V_b=11$ and $V_b=8$ are almost identical for the smallest coupling constant while it is not the case for $V_b=5$.

In the small coupling constant limit, the adiabatic potential-energy surface does not serve as a proper means for the understanding of the calculated nonadiabatic reaction rate. Figure 2 provides additional effective potential-energy surfaces as long dashed lines, which serve this purpose better. They are potential energies calculated along each instanton trajectory by the following expression:

$$V_{\mathrm{in}}(q)=V_{\mathrm{ad}}(q_b(0))+\int_{q_b(0)}^{q}dq'\langle V'(\tau_{q'})\rangle_{q_b(\cdot)}, \quad (31)$$

where $V_{\mathrm{ad}}(q_b(0))$ is the value of the lowest adiabatic potential-energy surface at the boundary of the instanton tra-

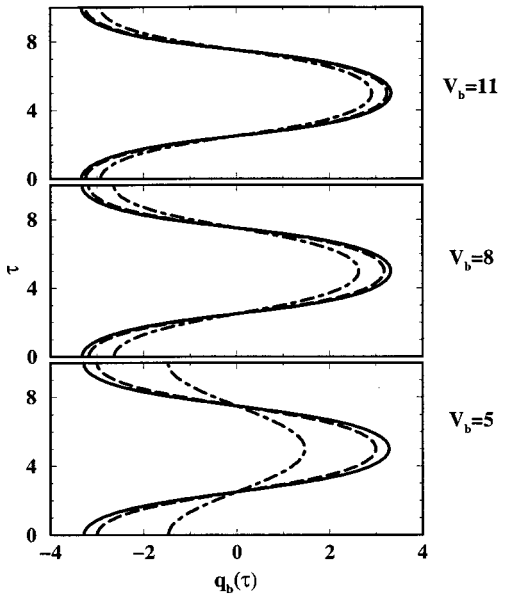


FIG. 3. Instanton trajectories for $\Delta=0.01$ (solid line), 2.37 (long dashed line), 4.0 (dotted–dashed line).

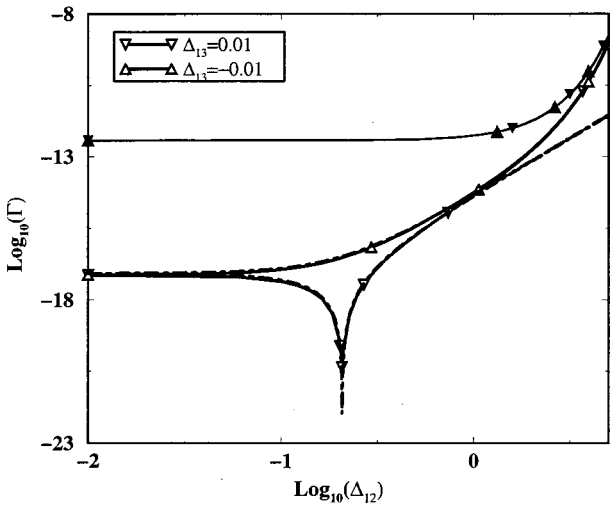


FIG. 4. Nonadiabatic instanton results (solid lines with open symbols) for a three state system with through–space coupling. Perturbation theory results are given by dotted-dashed lines and the adiabatic instanton results for the lowest surfaces are given by solid lines with corresponding filled symbols.

jectory, $q_b(0)$, and $\tau_{q'}$ is the imaginary time satisfying $q'=q_b(\tau_{q'})$. A time origin has been set such that $q_b(0)\leqslant q_b(\tau)\leqslant q_b(\beta\hbar/2)$. Thus, $V_{\rm in}(q)$ is a potential defined only within the bound of the instanton trajectory, and it reflects the amount of work required for the nuclear trajectory to tunnel through the barrier region. In all the three cases of $V_b$, $V_{\rm in}(q)$'s look quite similar in the weak electronic coupling limit. The reason for this is that quantum delocalization plays a bigger role and washes out the small details of the bare potential-energy surfaces.

Comparison of $V_{\rm in}(q)$ with the adiabatic potential surface in Fig. 2 shows that their relative difference can serve as a measure of nonadiabaticity as mentioned before.[48] For example, when $\Delta=0.01$, the two curves are substantially different in all three cases of $V_b$. When $\Delta=2.37$, they are quite close for the case of $V_b=5$, while the difference between the two curves for the case of $V_b=11$ is still large. Finally, when $\Delta=5$, one cannot discern the two potential energy surfaces for the cases of $V_b=8$ and 5, while a small difference can be seen for the case of $V_b=11$. These observations are all consistent with the crossover pattern shown in Fig. 1.

Figure 3 provides the actual nonadiabatic instanton trajectories. For the smallest coupling constant of $\Delta=0.01$, little difference can be seen between the instanton trajectories for different values of $V_b$, which reflects the similarity of the effective potentials calculated by Eq. (31). On the other hand, for the largest coupling constant of $\Delta=5$, the extent of the instanton trajectory for $V_b=5$ is much smaller than other cases. This is also consistent with the shape of the potential shown for the case of $V_b=5$ and $\Delta=5$ in Fig. 2, which has much smaller curvature than others.

### B. Three states system with through–space coupling

In the present subsection, the effect of the direct coupling between states $|1\rangle$ and $|3\rangle$, the so called through–space coupling, is considered. Thus the present model corresponds to the case of symmetric ET with both bridge mediation and through–space coupling. Recent examples show that such situations can occur for large flexible molecules[63] or for the case where there is an additional functional group in the bridge compound.[64] Interference effects can be important in this case. We assume the form of $\hat{H}_0$ of Eq. (4) as

$$\hat{H}_0=\frac{\hat{p}^2}{2m}\hat{I}+\Delta_{12}(|1\rangle\langle 2|+|2\rangle\langle 1|+|2\rangle\langle 2|+|3\rangle\langle 2|)+\Delta_{13}(|1\rangle\langle 3|+|3\rangle\langle 1|), \tag{32}$$

which corresponds to the simplest extension of the Hamiltonian given in the previous subsection. The same diabatic potentials, units, and value of $q_0$ are used. In order to focus more on the effect of the through–space coupling, we consider here only the case of $V_b=11$.

In the small coupling constant limit, the qualitative feature of the nonadiabatic reaction rate can be inferred from perturbation theory. Considered up to second order, the transition probability from $|1\rangle$ to $|3\rangle$ has two contributions of a direct transition and an indirect one via the intermediate state of $|2\rangle$. The probability of the former event is proportional to $|\Delta_{13}|^2$ and that of the latter is to $|\Delta_{12}|^4/V_b^2$, when considered independently. If there is a large disparity in the magnitudes of $|\Delta_{13}|$ and $|\Delta_{12}|^2/V_b$, independent consideration can be justified and only the dominant one will govern the overall reaction rate. However, when they are comparable, their contributions should be considered on the same footing and the reaction rate can be sensitive to their relative phase. The major concern here is whether the nonadiabatic instanton theory can correctly reproduce this qualitative feature. If it does, then, the next question is how the theory predicts interference effects in the moderately large coupling constant regime where the perturbation theory does not work well.

In order to answer the first question, we performed calculations for the two cases of $\Delta_{13}=\pm 0.01$, a weak through–

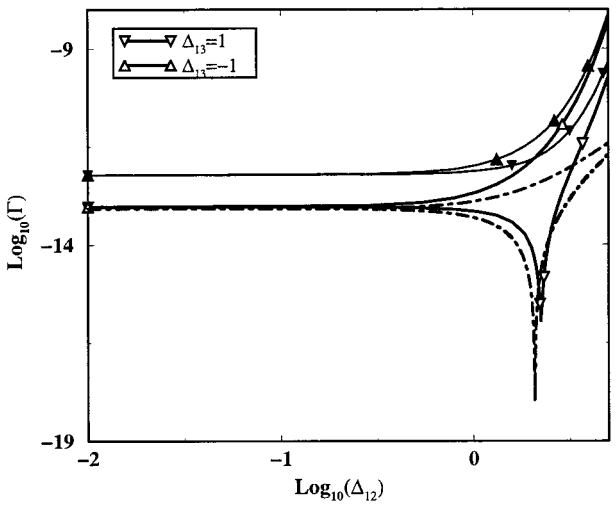


FIG. 5. Nonadiabatic instanton results (solid lines with open symbols) for a three system with through–space coupling. Perturbation theory results are given by dotted-dashed lines and the adiabatic instanton results for the lowest surfaces are given by solid lines with corresponding filled symbols.

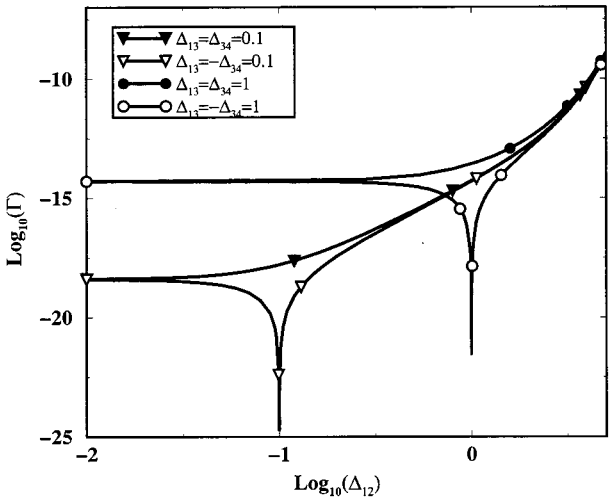


FIG. 6. Nonadiabatic instanton results for a four states system with two degenerate bridge states.

space coupling limit. Figure 4 shows the results. A striking interference effect can be seen, and the nonadiabatic instanton theory agrees fairly well with the second order perturbation theory results, calculated as described in Appendix B. Because $\epsilon_l - \epsilon_m < 0$ in Eq. (B4), one can see that the negative value of $\Delta_{31}$ results in constructive interference, while the positive sign leads to destructive one. As $\Delta_{12}$ increases, on the other hand, the results of the nonadiabatic instanton theory, for both cases of $\Delta_{13} = \pm 0.01$, approach those of the adiabatic instanton theory, which are almost equal for the present case. These confirm that the theory reproduces a correct interference pattern and approaches both the weak and strong coupling limits properly.

In order to address the next question, we performed calculations for $\Delta_{13} = \pm 1$, cases with moderately large through–space coupling constants. The results are shown in Fig. 5. Interestingly, a qualitative feature similar to that of the perturbation theory can be seen, but the value of $\Delta_{12}$ where the interference is maximized appears somewhat later. Although the perturbation theory provides a qualitatively correct picture, actual nonadiabatic calculation is necessary for an accurate quantification of the reaction rate. In the present case, the two adiabatic instanton theory results also show substantial difference, and the two results of the nonadiabatic instanton theory approach these different adiabatic ones in the limit of large through–bond coupling constant.

Two important aspects are worth stressing. First, in the presence of additional through–space coupling, the increase of the through bond coupling does not always lead to the increase of the reaction rate for the case of destructive interference. Second, the variation of the phase of the through–space coupling, or that of only one through–bond coupling, can be a very efficient means for the control of the overall reaction rate. Whether such an effect can be found in nature or in experiments is not so clear, but, as recent calculations[65] for photosynthetic reaction center suggest, proper account of all the coupling constants should be an important factor in correct quantification of the reaction rate in multistate systems.

### C. Four states system

Finally, calculations for a four states model system are made, mainly to examine whether similar interference effects can be found. The model is assumed to have two bridge states, $|2\rangle$ and $|3\rangle$, which are not coupled to each other, but are coupled to the donor state, $|1\rangle$, and the acceptor state, $|4\rangle$, independently. Thus,

$$\hat{H}_0 = \frac{\hat{p}^2}{2m}\hat{I} + \Delta_{12}(|1\rangle\langle 2| + |2\rangle\langle 1|) + \Delta_{12}(|2\rangle\langle 4| + |4\rangle\langle 2|) + \Delta_{13}(|1\rangle\langle 3| + |3\rangle\langle 1|) + \Delta_{34}(|3\rangle\langle 4| + |4\rangle\langle 3|), \quad (33)$$

where it is assumed that the coupling between $|2\rangle$ and $|4\rangle$ is the same as that between $|1\rangle$ and $|2\rangle$. On the other hand, the coupling between $|1\rangle$ and $|3\rangle$ is not necessarily the same as that between $|3\rangle$ and $|4\rangle$. In order to emphasize the interference effect, we assume that the potential-energy surfaces of $|2\rangle$ and $|3\rangle$ are the same, as in some model systems of PCET reaction.[8] That is, the diabatic potential-energy surfaces are given by

$$V_1(q) = \frac{m\omega^2}{2}(q + q_0)^2, \quad (34)$$

$$V_2(q) = V_3(q) = \frac{m\omega^2}{2}q^2 + V_b, \quad (35)$$

$$V_4(q) = \frac{m\omega^2}{2}(q - q_0)^2, \quad (36)$$

where $q_0 = 4$ as before, and $V_b$ was chosen to be 11. Calculations were done as described in Appendix A with the same set of parameters, except that there are now four electronic states. Figure 6 shows the phase effects for both small and large magnitudes of $|\Delta_{13}| = |\Delta_{34}|$, with the variation of $\Delta_{12}$.

Interference effects similar to three states systems can be seen. In the present case, the maximum interference appears

when the absolute value of $\Delta_{12}$ is equal to that of $\Delta_{13}$, because both processes involving $|2\rangle$ and $|3\rangle$ are of second order. The degrees of interference are similar for both small and large magnitudes of $|\Delta_{13}|=|\Delta_{34}|$. Although the model considered here is too simplistic, it has some relevance to PCET in the low-temperature regime, where excited proton states can be disregarded and the polarization coordinate behave quantum mechanically. The present calculation suggests substantial interference effect for such a situation. Experimental verification of this might be possible for well designed synthetic systems.

## IV. DISCUSSION

In this paper, the nonadiabatic instanton theory was successfully applied to three and four states systems and was shown to account for electronic interference effects. Within our knowledge, this is the first demonstration of such effects from the perspective of instanton theory. For the chosen set of parameters, the difference in the reaction rate, between the constructive and destructive interference cases, is about five orders of magnitudes. Even though this large difference were not observed in actual situations, it still illustrates that neglecting through–space couplings or additional through–bond channels can result in substantial overestimation or underestimation of actual reaction rate.

In the present work, calculations were limited to simple one-dimensional model systems in order to emphasize the unique features of multistate systems. However, application to more general and realistic situations are possible, and can reveal new interesting aspects. First, one can consider more general shapes of potential-energy surfaces and study the role of anharmonicity and the effects of different curvatures for different electronic states. Second, it is possible to consider the cases where the nuclear reaction coordinate is coupled to bath modes, with the use of relevant influence functional.[48,49] Third, applications to systems with two-dimensional nuclear coordinates are possible, and these can demonstrate different behavior depending on the topology of the potential-energy surfaces. For two-dimensional cases, there can be more than one instanton trajectories connecting the reactant and the product states. In addition, more various routes of sequential mechanisms are possible. Considerations of all these possibilities and determination of the dominant one(s) are essential in determining the reaction mechanism of a give system.

The reaction rate considered in the present work corresponds to coherent concerted mechanism, which does not allow thermal relaxation of the intermediate states. For multistate systems, however, there are other competing routes of sequential mechanisms where the intermediate states are actually populated and fully relaxed. Within the instanton approach, it is also possible to calculate the reaction rates of these sequential mechanisms by performing separate instanton calculations for each pair of potential-energy surfaces involved in each step of the sequential mechanism and then calculating the overall reaction rate combining those of all the steps involved.

As is usual for instanton theory, the nonadiabatic instanton theory presupposes sufficiently low temperature as illustrated in the beginning of Sec. III. In addition, it has been assumed that there exists a well defined reaction coordinate that can be used to monitor the progress of reaction. Therefore, the examples where the present theory is suitable are low-temperature intramolecular ET with distinctive reactant and product configurations, bridge mediated ET where there is a well defined polarization coordinate serving as a quantum reaction coordinate, and PCET reactions with a significant tunneling of the proton coordinate.

Finally, we conclude the paper with a few comments on theoretical and numerical issues which need further attention. First, no clear criterion for the existence of the instanton trajectory has been found yet. That is, an explicit expression for the crossover temperature does not exist, unlike in the adiabatic instanton theory. This makes it difficult to assess whether a given system is in the proper regime for the application of the instanton theory before the calculation is performed. A possible way to go around this ambiguity is to utilize the nonadiabatic centroid.[66] Second, for the case of a real time propagator, it is known that there can be multiple stationary paths.[67] Whether the same is true and whether it can play an important role for the present situation of imaginary time propagation are not clear at this point. Third, the numerical method of finding an instanton trajectory as described in Appendix A has been successful in most parameter regime of the models considered, but there are some limiting situations where the method does not work well, which are detailed in Appendix A. The main conclusion of the present paper is hardly affected by this numerical issue, but further understanding and possible improvement of the numerical algorithm is important for future applications of the theory to real systems.

## ACKNOWLEDGMENTS

S.J. thanks Dr. C. Schwieters for very informative discussions. This work was supported by grants from Research Corporation, Petroleum Research Fund, and National Science Foundation.

## APPENDIX A: NUMERICAL METHOD

In actual calculation, the limit of $N\rightarrow\infty$ is not taken, and one assumes a finite but large enough $N$. Correspondingly, the imaginary time of $\tau$ can take only discrete values, $\tau_j = j\epsilon$, and the electronic influence functional operator defined by Eq. (8) is approximated by a finite number of products as follows:

$$\hat{J}[q(\cdot);\tau_{j'},\tau_{j''}]\approx\hat{J}(q_{j'},q_{j'+1};\epsilon)\cdots\hat{J}(q_{j''-1},q_{j''};\epsilon). \tag{A1}$$

Also, the ''classical'' equation of motion, Eq. (16), is replaced with the following finite difference equation:

$$q_{0,j+1}-2q_{0,j}+q_{0,j-1}=\frac{\epsilon^2}{m}\langle V'(\tau_j)\rangle_{q_0(\cdot)}, \tag{A2}$$

where $q_{0,j}=q_0(\tau_j)$. Finally, the eigenvalues entering Eq. (1) are approximated by those of the $N\times N$ matrix $\mathbf{D}_\epsilon[q_0(\cdot)]$, a finite $N$ approximation for the operator defined by Eq. (18), the component of which is given by

$$(\mathbf{D}_\epsilon[q_0(\cdot)])_{j,j'} = -\frac{m}{\epsilon^2}(\delta_{j,j'-1} - 2\delta_{j,j'} + \delta_{j,j'+1}) + \langle V''(\tau_j)\rangle_{q_0(\cdot)}\delta_{j,j'} - \frac{\beta}{N}C[q_0(\cdot);\tau_j,\tau_{j'}], \tag{A3}$$

where $j,\ j' = 0,...,N-1$. When these discretized approximations are inserted into Eq. (26), the resulting rate expression is equivalent to that provided by SV.[50]

Since the righthand side of Eq. (A2) depends implicitly on the trajectory *to be determined*, a self-consistent approach is needed in the calculation of the instanton trajectory. A simple way for this is an iteration procedure described as follows: (i) Choose a reasonable initial guess for the instanton trajectory; (ii) calculate the electronic influence functional operator along the given trajectory using Eq. (A1); (iii) solve the equation of motion, Eq. (A2), iteratively employing the electronic influence functional as determined by the step of (ii); (iv) use the trajectory determined in step (iii) as a new input and repeat the steps (ii) and (iii) until enough convergence is reached. In step (iii), the iteration is done by repeating the following cycle of update:

$$2q_{0,j}^{\text{new}} = q_{0,j+1}^{\text{old}} + q_{0,j-1}^{\text{old}} - \frac{\epsilon^2}{m}\langle V'(\tau_j)^{\text{old}}\rangle_{q_0(\cdot)}, \quad j = 0,...,N-1, \tag{A4}$$

until enough convergence is achieved. In the calculations for the model systems in the text, the update of Eq. (A4) was done 100 times at each step.

The iteration procedure described above, which will be named as ITER hereafter, has quite a simple structure. However, the convergence of the procedure is very slow in general, and sometimes a desired convergence is not reached at all. Alternatively, one can use a more systematic Newton–Rapson (NR) procedure as applied by SV,[50] which accounts for the dependence of the electronic influence functional on the nuclear trajectory simultaneously. Although, each step of the NR procedure takes longer than ITER, the overall convergence of NR is faster than ITER. However, for some cases, the NR procedure leads to instability and does not produce a trajectory with enough convergence. We found that augmenting the NR procedure with the ITER procedure can prevent such a problematic situation from happening in most cases. Thus, the following is the overall algorithm we adopted in finding the nonadiabatic instanton solution: (i) Choose the straight line solution connecting the minima of the reactant and product state potential as the initial trajectory; (ii) calculate the electronic influence functional operator; (iii) apply the NR procedure; (iv) apply the steps (ii) and (iii) of the ITER procedure twice. The steps from (i) to (iv) described here constitute our composite method of finding the nonadiabatic instanton solution. We repeated the steps from (ii) to (iv) until the measure of convergence defined as

$$C = \frac{1}{N}\sum_j \left| q_{0,j+1} - 2q_{0,j} + q_{0,j-1} - \frac{\epsilon^2}{m}\langle V'(\tau_j)\rangle_{q_0(\cdot)} \right|^2, \tag{A5}$$

becomes small enough. In the calculations of the main text, the upper bound of $C$ was set to $1\times10^{-14}$.

For a given model system, calculations were made at 20 values of the varying through–bond coupling constant, uniformly spaced in the given interval, except for the cases of destructive interference. For these latter cases, more points were needed near the minimum in order to reproduce smoothly the dip in the reaction rate. As the coupling constant approaches the value where the reaction rate becomes minimum, however, we found it difficult to obtain the desired convergence. The results shown in the texts are for only those points with convergences within the bound set above. Thus, the minimum value of the reaction rate for the cases of destructive interferences might have some errors.

## APPENDIX B: SECOND-ORDER PERTURBATION THEORY EXPRESSION AND ITS CALCULATION

Here, we derive an expression for the general three state systems where there are both through–space ($\Delta_{13}$) and through–bond ($\Delta_{12}$ and $\Delta_{23}$) couplings. When considered up to the second-order time-dependent perturbation theory, the electronic space matrix element of the propagator is given by

$$\langle 3|e^{-i\hat{H}t/\hbar}|1\rangle = -\frac{i}{\hbar}\int_0^t dt' e^{-i\hat{h}_3(t-t')/\hbar}\Delta_{31}e^{-i\hat{h}_1 t'/\hbar} - \frac{1}{\hbar^2}\int_0^T dt'\int_0^{t'} dt'' e^{-i\hat{h}_3(t-t')/\hbar}\Delta_{32} \times e^{-i\hat{h}_2(t-t'')/\hbar}\Delta_{21}e^{-i\hat{h}_1 t''/\hbar}. \tag{B1}$$

We denote the diabatic vibrational states of the electronic states of 1, 2, and 3 as $|l\rangle$, $|m\rangle$, and $|n\rangle$, respectively. Then

$$\langle n|\langle 3|e^{-i\hat{H}t/\hbar}|1\rangle|l\rangle = -\frac{i}{\hbar}\Delta_{31}\int_0^t dt' e^{-i\epsilon_n(t-t')/\hbar - i\epsilon_l t'/\hbar}\langle n|l\rangle - \frac{\Delta_{32}\Delta_{21}}{\hbar^2} \times \int_0^t dt'\int_0^{t'} dt'' \sum_m e^{-i\epsilon_n(t-t')/\hbar} \times e^{-i(\epsilon_m - i\gamma)(t'-t'')/\hbar - i\epsilon_l t''/\hbar}\langle n|m\rangle\langle m|l\rangle, \tag{B2}$$

where $\gamma\to 0+$. Performing integration over $t''$, one can show that

$$e^{i\epsilon_n t/\hbar}\langle n|\langle 3|e^{-i\hat{H}t/\hbar}|1\rangle|l\rangle = -\frac{i}{\hbar}\int_0^t dt' e^{i(\epsilon_n - \epsilon_l)t'/\hbar} \times \left(\Delta_{31}\langle n|l\rangle + \Delta_{32}\Delta_{21}\sum_m \frac{\langle n|m\rangle\langle m|l\rangle}{\epsilon_l - \epsilon_m + i\gamma}\right), \tag{B3}$$

where it has been assumed that $e^{i(\epsilon_l - \epsilon_m + i\gamma)t'/\hbar} \ll 1$.

Taking the absolute square of Eq. (B3) and the time derivative, summation over all the final electronic states gives rise to the following expression for the transition rate from the $l$ vibrational state of the donor electronic state to the acceptor state:

$$k_l=\frac{2\pi}{\hbar}\rho_3(\epsilon_l)\left|\Delta_{31}\langle n_l|l\rangle+\Delta_{32}\Delta_{21}\sum_m \frac{\langle n_l|m\rangle\langle m|l\rangle}{\epsilon_l-\epsilon_m+i\gamma}\right|^2, \quad \text{(B4)}$$

where $n_l$ is the vibrational state of the electronic state of $|3\rangle$ such that $\epsilon_{n_l}=\epsilon_l$. For the model systems considered in the text, $\rho_3(\epsilon_l)=1/(\hbar\omega)$. The final expression for the reaction rate is then given by

$$k=\frac{1}{Z_1}\sum_l e^{-\beta\epsilon_l}k_l, \quad \text{(B5)}$$

where $Z_1=\Sigma_l e^{-\beta\epsilon_l}$. In the calculation, the summations were truncated at $l=3$ and $m=60$. For the choice of parameters given in the text, consideration only up to $l=3$ excludes the resonance transfer. The assumption behind this truncation is that the thermal weights for the higher possible resonant states are much smaller than the resonance enhancement factor of $1/|\gamma|^2$.


[1] J. Jortner and M. Bixon, *Adv. Chem. Phys., Vol. 106, Parts 1 and 2: Electron Transfer From Isolated Molecules to Biomolecules* (Wiley, New York, 1999).
[2] P. Chen and T. J. Meyer, Chem. Rev. **98**, 1439 (1998).
[3] G. Iversen, E. P. Friis, Y. Kharkats, A. M. Kuznetsov, and J. Ulstrup, J. Bio. Inorg. Chem. **3**, 229 (1998).
[4] D. Gust, T. A. Moore, and A. L. Moore, Acc. Chem. Res. **26**, 198 (1993).
[5] N. W. Woodbury, S. Lin, X. Lin, J. M. Peloquin, A. K. W. Taguchi, J. C. Willians, and J. A. Allen, Chem. Phys. **197**, 405 (1995).
[6] M. S. Graige, M. L. Paddock, J. M. Bruce, G. Fehr, and M. Y. Okamura, J. Am. Chem. Soc. **118**, 9005 (1996).
[7] R. Schmid and A. Labahn, J. Phys. Chem. B **104**, 2928 (2000).
[8] R. I. Cukier and D. G. Nocera, Annu. Rev. Phys. Chem. **49**, 337 (1998).
[9] A. C. Reddy, D. Danovich, A. Ioffe, and S. Shaik, J. Chem. Soc., Perkin Trans. 1 **2**, 1525 (1995).
[10] E. Fernandez, L. Blancafort, M. Olivucci, and M. A. Robb, J. Am. Chem. Soc. **122**, 7528 (2000).
[11] A. Cheong, A. E. Roitberg, V. Mujica, and M. A. Ratner, J. Photochem. Photobiol., A **82**, 81 (1994).
[12] M. J. Shephard and M. N. Paddon-Row, J. Phys. Chem. **99**, 17494 (1995).
[13] C. Patoux, C. Coudret, J.-P. Launay, C. Joachim, and A. Gourdon, Inorg. Chem. **36**, 5037 (1997).
[14] C. Turro, C. K. Chang, G. E. Leroi, R. I. Cukier, and D. G. Nocera, J. Am. Chem. Soc. **114**, 4013 (1992).
[15] J. A. Roberts, J. P. Kirby, and D. G. Nocera, J. Am. Chem. Soc. **117**, 8051 (1995).
[16] J. P. Kirby, J. A. Roberts, and D. G. Nocera, J. Am. Chem. Soc. **119**, 9230 (1997).
[17] R. I. Cukier, J. Phys. Chem. **98**, 2377 (1994).
[18] R. I. Cukier, J. Phys. Chem. **99**, 16101 (1995).
[19] R. I. Cukier, J. Phys. Chem. **100**, 15428 (1996).
[20] A. Soudackov and S. Hammes-Schiffer, J. Chem. Phys. **111**, 4672 (1999).
[21] A. Soudackov and S. Hammes-Schiffer, J. Chem. Phys. **113**, 2385 (2000).
[22] H. Decornez and S. Hammes-Schiffer, J. Phys. Chem. A **104**, 9370 (2000).
[23] L. Roecker and T. J. Meyer, J. Am. Chem. Soc. **108**, 4066 (1986).
[24] R. A. Binstead, M. E. McGuire, A. Dovletoglous, W. K. Seok, L. E. Roecker, and T. J. Meyer, J. Am. Chem. Soc. **114**, 173 (1992).
[25] B. T. Farrer and H. H. Thorp, Inorg. Chem. **38**, 2497 (1999).
[26] M. H. V. Huynh, T. J. Meyer, and P. S. White, J. Am. Chem. Soc. **121**, 4530 (1999).
[27] L. D. Zusman, Chem. Phys. **49**, 295 (1980).
[28] M. Sparpaglione and S. Mukamel, J. Chem. Phys. **88**, 3263 (1988).
[29] X. Song and A. A. Stuchebrukhov, J. Chem. Phys. **99**, 969 (1993).
[30] J. Stockburger and C. H. Mak, J. Chem. Phys. **105**, 8126 (1996).
[31] Y. Jung, R. J. Silbey, and J. Cao, J. Phys. Chem. A **103**, 9460 (1999).
[32] J. Cao and Y. Jung, J. Chem. Phys. **112**, 4716 (2000).
[33] J. Tang, Chem. Phys. **184**, 39 (1994).
[34] A. Kimura and T. Kakitani, Chem. Phys. Lett. **298**, 241 (1998).
[35] T. Bandyopadhyay, A. Okada, and M. Tachiya, J. Chem. Phys. **110**, 9630 (1999).
[36] L. D. Zusman and D. N. Beratan, J. Chem. Phys. **110**, 10468 (1999).
[37] N. Makri, Annu. Rev. Phys. Chem. **50**, 167 (1999).
[38] R. Egger and C. H. Mak, J. Phys. Chem. **98**, 9903 (1994).
[39] P. Pechukas, Phys. Rev. **181**, 166 (1969).
[40] M. Ben-Nun and T. J. Martinez, J. Chem. Phys. **108**, 7244 (1998).
[41] G. Stock and M. Thoss, Phys. Rev. Lett. **78**, 578 (1997).
[42] X. Sun, H. Wang, and W. H. Miller, J. Chem. Phys. **109**, 7064 (1998).
[43] A. Donoso and C. C. Martens, J. Chem. Phys. **112**, 3980 (2000).
[44] H. S. Mei and D. F. Coker, J. Chem. Phys. **104**, 4755 (1996).
[45] O. V. Prezhdo and P. J. Rossky, J. Chem. Phys. **107**, 825 (1997).
[46] C. C. Martens and J.-Y. Fang, J. Chem. Phys. **106**, 4918 (1997).
[47] D. Sholl and J. C. Tully, J. Chem. Phys. **109**, 7702 (1998).
[48] J. Cao, C. Minichino, and G. A. Voth, J. Chem. Phys. **103**, 1391 (1995).
[49] J. Cao and G. A. Voth, J. Chem. Phys. **106**, 1769 (1997).
[50] C. D. Schwieters and G. A. Voth, J. Chem. Phys. **108**, 1055 (1998).
[51] W. H. Miller, J. Chem. Phys. **62**, 1899 (1975).
[52] J. C. G. Callan and S. Coleman, Phys. Rev. D **16**, 1762 (1977).
[53] S. Coleman, Phys. Rev. D **15**, 2929 (1977).
[54] I. Affleck, Phys. Rev. Lett. **46**, 388 (1981).
[55] V. A. Benderskii, V. I. Goldanskii, and D. E. Makarov, Phys. Rep. **233**, 195 (1993).
[56] T. Nakamura, A. Ottewill, and S. Takagi, Ann. Phys. **87**, 9 (1997).
[57] J. Cao and G. A. Voth, J. Chem. Phys. **105**, 6856 (1996).
[58] A. O. Caldeira and A. J. Leggett, Phys. Rev. Lett. **46**, 211 (1981).
[59] A. O. Caldeira and A. J. Leggett, Ann. Phys. **149**, 374 (1983).
[60] T. R. Holstein, Philos. Mag. B **37**, 49 (1978).
[61] J. P. Sethna and S. Kivelson, Phys. Rev. B **26**, 3513 (1982).
[62] P. G. Wolynes, J. Chem. Phys. **86**, 1957 (1986).
[63] F. C. De Schryver, D. Declercq, S. Depaemelaere, E. Hermans, A. Onkelinx, J. W. Verhoeven, and Gelan, J. Photochem. Photobiol., A **82**, 171 (1994).
[64] A. M. Napper, I. Read, and D. H. Waldeck, J. Am. Chem. Soc. **122**, 5220 (2000).
[65] D. Kolbasov and A. Scherz, J. Phys. Chem. B **104**, 1802 (2000).
[66] C. D. Schwieters and G. A. Voth, J. Chem. Phys. **111**, 2869 (1999).
[67] J. L. McWhirter, J. Chem. Phys. **110**, 4184 (1999).